Electronic Supplementary Material (ESI) for Nanoscale.

SUPPLEMENTARY INFORMATION

Supplementary Figures S1-S11

Supplementary Table S1

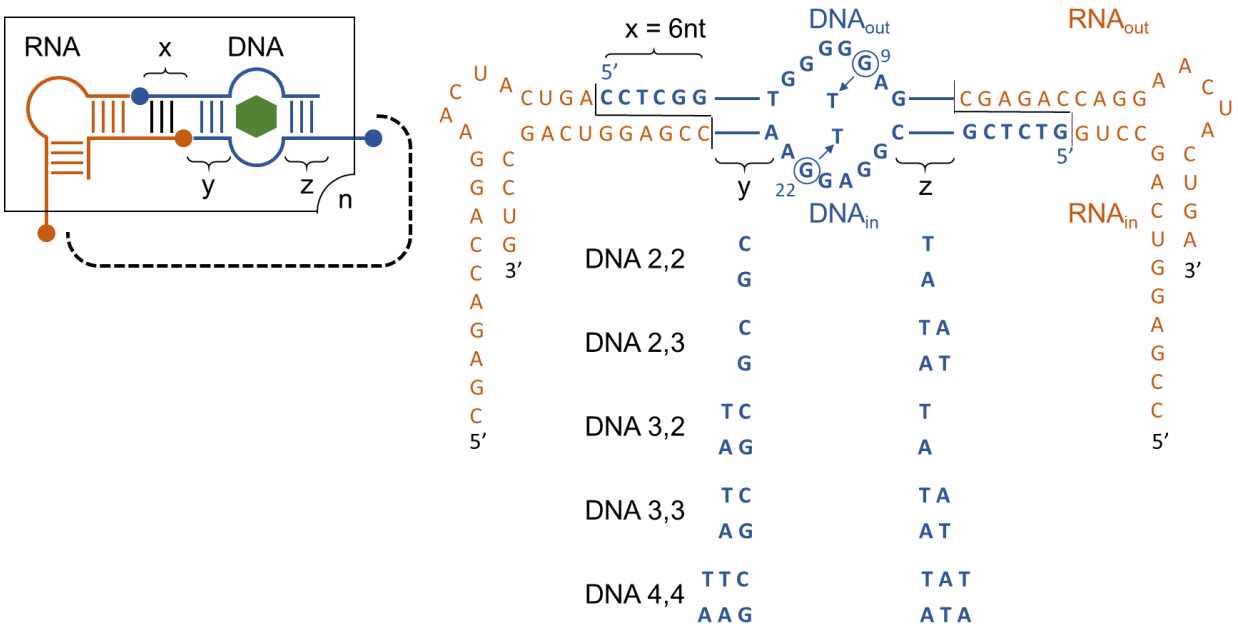

Fig. S1. Design of ligand-dependent RNA-DNA hybrid nanoshapes. RNA corner modules (orange) are derived from the subdomain IIa internal loop of the hepatitis C virus (HCV) internal ribosome entry site (IRES), which was previously used to construct a self-assembling all-RNA nanosquare. A series of DNA module inserts (blue) was designed that carried an internal loop sequence of an AMP aptamer flanked by double-stranded regions (y, z) of 2-4 base pairs (bp). RNA corner modules and DNA inserts each contain complementary 5' single-stranded overhangs (x) of 6 nucleotides (nt) which allow for self-assembly through inter-strand base pairing. Single-stranded overhangs within modules have distinct sequences (indicated by green and blue color) to prevent formation of homomeric assemblies. Base changes introduced at positions G9 and G22 in some of the constructs are indicated (see also Fig. 2B). See ESI Table S1 for a complete list of all oligonucleotides used in this research.

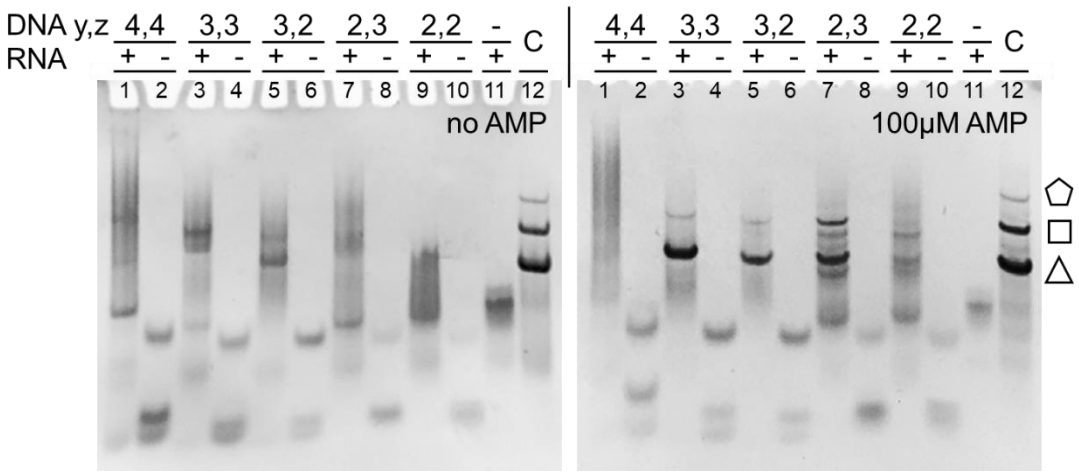

Fig. S2. PAGE analysis of combinations of an RNA corner motif and variants of an AMP-binding DNA aptamer module in the presence of 5 mM magnesium ions. Gel execution and sample arrangement are identical to the gels shown in Fig. 2A, except for the higher magnesium concentration. Stable RNA-DNA hybrid nanoshapes give rise to discrete bands without leaving nucleic acid material retained in the gel pocket. DNA aptamer modules were tested that contain single-stranded overhangs (x) of 6 nucleotides and different lengths of the double stranded regions (y, z) flanking the AMP-binding loop (see ESI Fig. S1 for sequences). PAGE analysis of the RNA-DNA module combinations was performed on two separate gels, respectively, in the absence and presence of 100 µM AMP ligand. For each aptamer variant, the DNA module was tested by itself and in combination with the RNA corner motif (lanes 1-10). Control lanes show the RNA corner by itself (lane 11) and hybrid nanoshapes (C, lane 12) that contain the same RNA corner motif connected by a simple double-stranded DNA module of 11 base pairs flanked by 6-nucleotide single-stranded overhangs. Nanoshapes used for the control (C, lane 12) assemble as a mixture of polygons as previously confirmed by AFM.

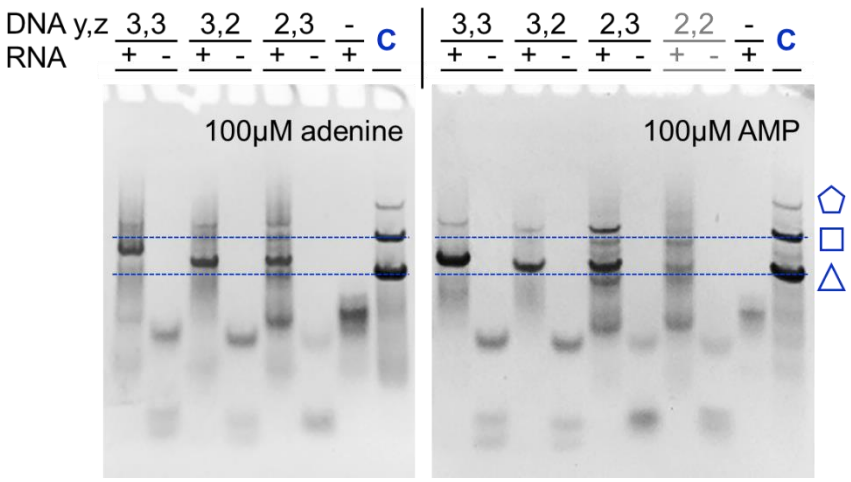

Fig. S3. PAGE analysis of hybrid nanoshapes containing aptamer DNA variants in the presence of 100 µM adenine (left gel) compared to the same nanoshape preparations in the presence of 100 µM AMP (right gel). Sample preparation and PAGE analysis were performed on samples containing 5 mM magnesium ions for both gels. The analysis in the presence of AMP is shown for comparison (right gel) and is part of the gel image reproduced in ESI Fig. S2. Lanes marked by C show hybrid nanoshapes that contain the RNA corner motif connected by a simple double-stranded DNA module of 11 base pairs flanked by 6-nucleotide single-stranded overhangs.

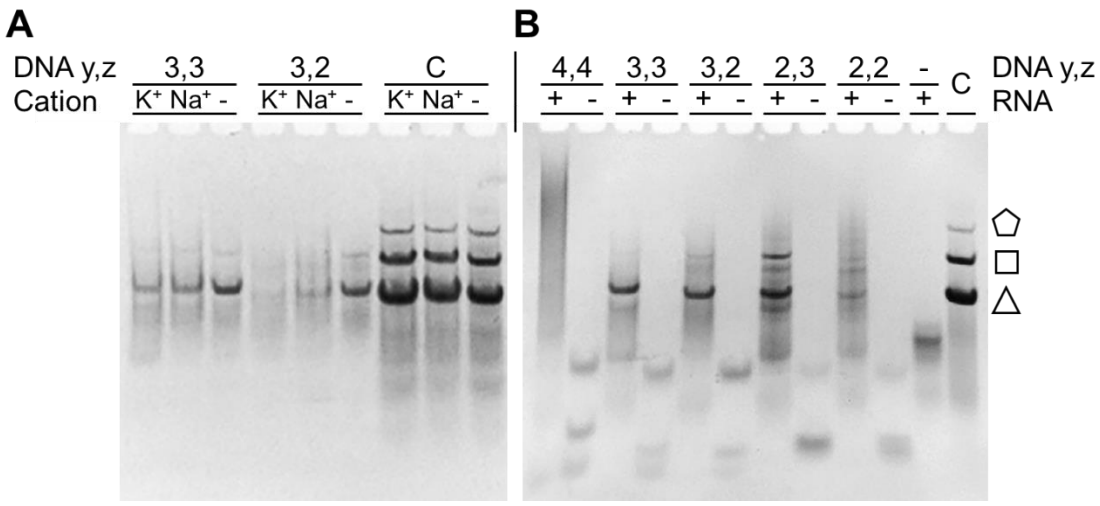

Fig. S4. Impact of monovalent cations on the formation of hybrid nanoshapes containing aptamer DNA variants in the presence of 100 μM AMP and 2 mM magnesium ions. **(A)** PAGE analysis of samples containing combinations of the RNA corner motif and AMP-binding DNA aptamer variants in the presence of 100 mM potassium or sodium ions. Monovalent ions were present in the sample preparation but not added to the gel or electrophoresis buffer. Lanes without monovalent ions indicated contain magnesium only. Lanes marked by C show hybrid nanoshapes that contain the RNA corner motif connected by a simple double-stranded DNA module of 11 base pairs flanked by 6-nucleotide single-stranded overhangs. **(B)** For comparison, a gel image from Fig. 2A is reproduced which shows PAGE analysis of hybrid nanoshapes containing DNA aptamer variants in the presence of 100 μM AMP ligand and 2 mM magnesium ions.

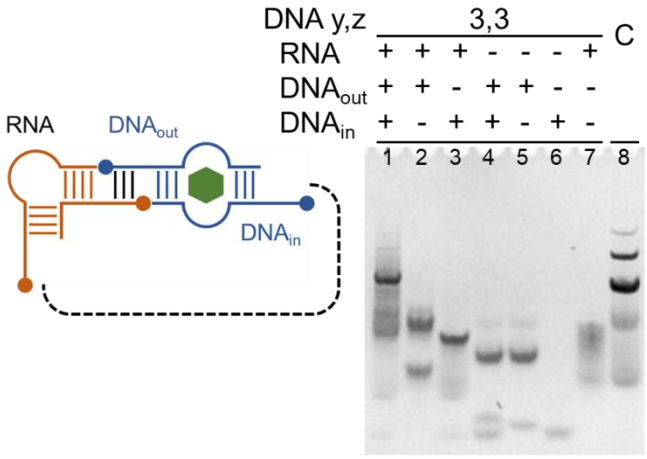

Fig. S5. PAGE analysis of nucleic acid components that were used to assemble RNA-DNA hybrid nanoshapes containing the DNA 3,3 aptamer module in the presence of 100 μM AMP ligand. Aptamer DNA insert was tested as individual strands (lanes 5, 6) and as DNA duplex (lane 4) in comparison with combinations of the DNA components with the RNA corner motif (lanes 1, 2, 3). RNA corner by itself is applied in lane 7. Lane 8 (C) shows hybrid nanoshapes that contain the same RNA corner motif connected by a simple double-stranded DNA module of 11 base pairs flanked by 6-nucleotide single-stranded overhangs.

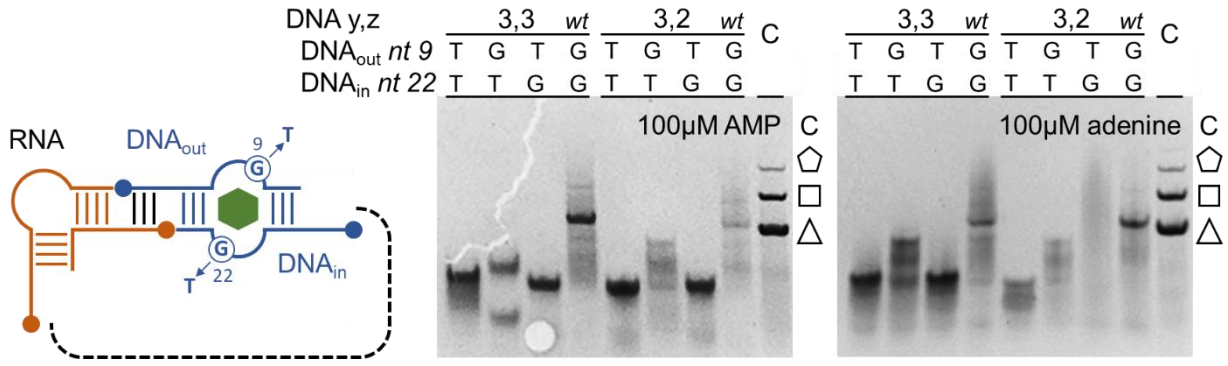

Fig. S6. PAGE analysis of nanoshapes that contain mutated DNA aptamer modules carrying single or double base changes (G→T) at positions 9 and 22 of the AMP binding loop which ablate ligand recognition. Mutation at either position prevent formation of the nanoshapes in the presence of AMP (left gel) or adenine (right gel). See also Fig. 2B from which the AMP gel is reproduced here. For reference, a control lane is included (C) to show similarly-shaped size markers, consisting of hybrid nanoshapes that contain the same RNA corner motif connected by a simple double-stranded DNA module of 11 base pairs flanked by 6-nucleotide single-stranded overhangs. Nanoshapes used for the control (C) assemble as a mixture of polygons as previously confirmed by AFM.

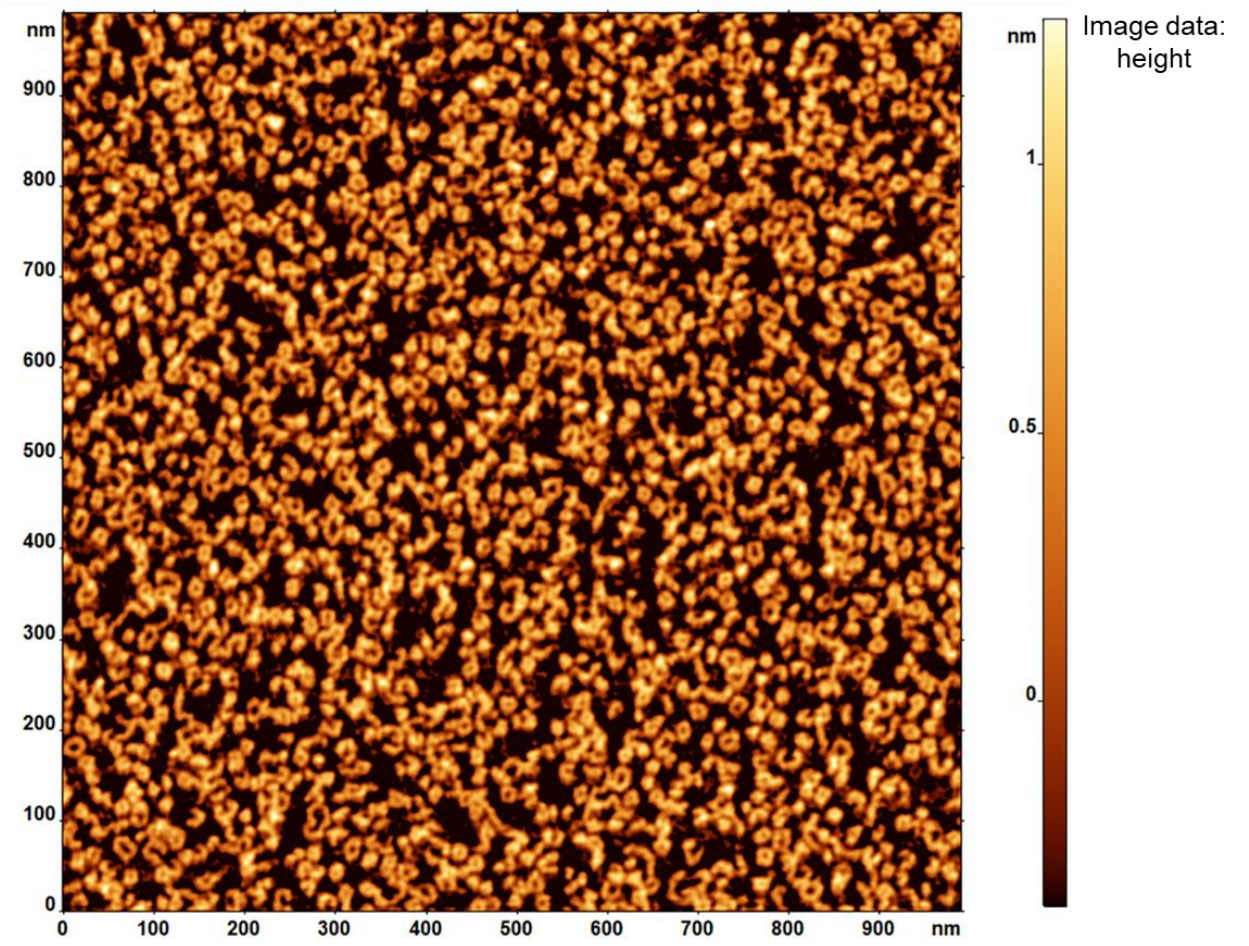

Fig. S7A. AFM imaging field of ligand-dependent RNA-DNA hybrid nanoshapes. Imaging was performed on nanoshapes obtained from combination of the RNA corner motif and DNA 3,3 aptamer module in the presence of 100 μM AMP ligand and 2 mM magnesium salt. See also Fig. 3.

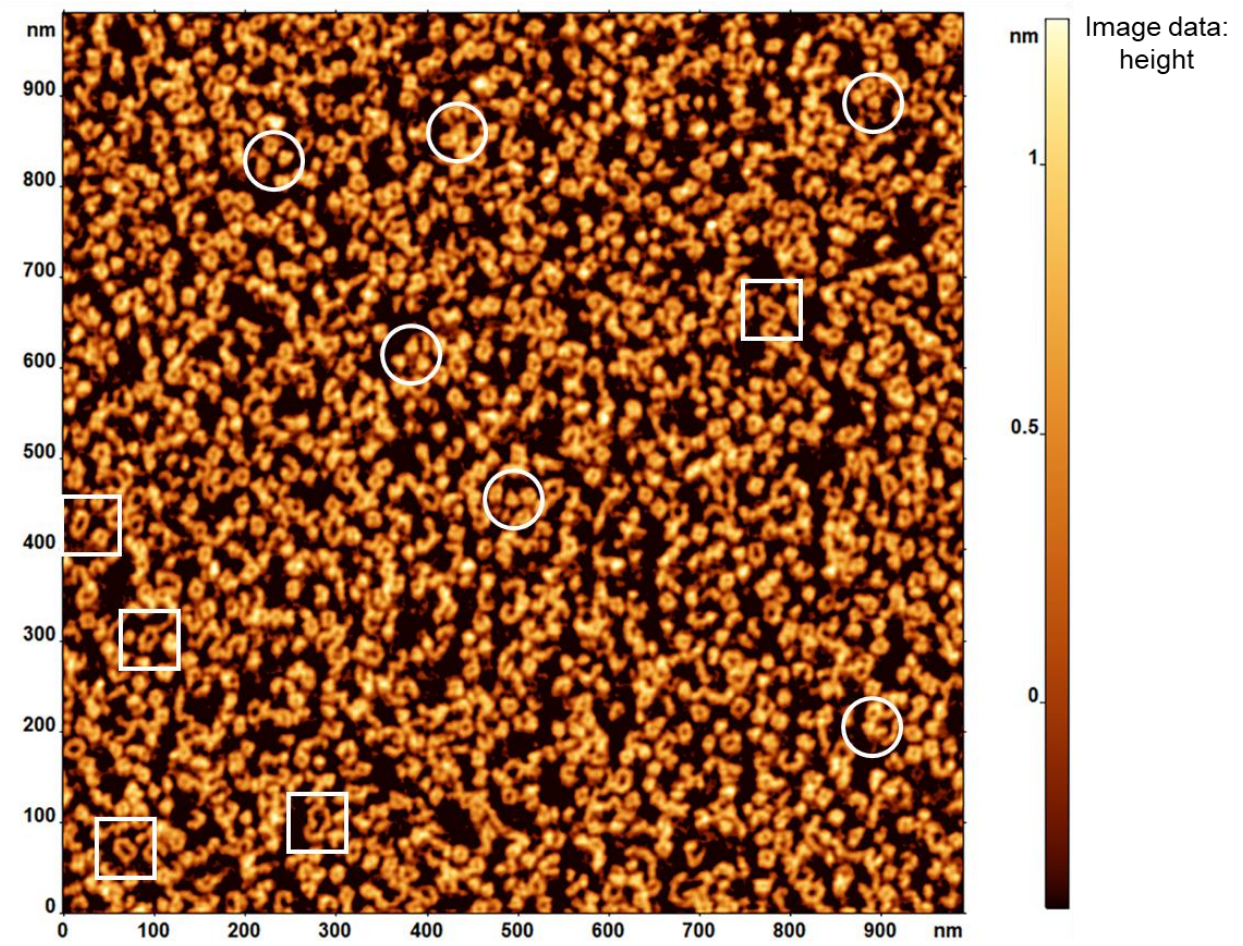

Fig. S7B. AFM imaging field of ligand-dependent RNA-DNA hybrid nanoshapes as shown also in ESI Fig. S7A. Here, nanotriangles are highlighted with circles and larger polygons marked by squares.

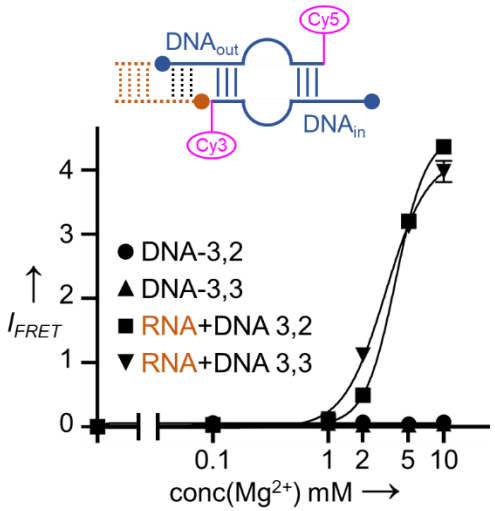

Fig. S8. FRET response in titration of fluorescently labeled nanoshape component mixtures with $MgCl_2$. Mixtures contained DNA aptamer variant strands with the FRET dye pair Cy3/Cy5 attached at the 3' terminus of, respectively, DNA_{in} and DNA_{out} (DNA 3,2 ● and DNA 3,3 ▲), and the same DNA strands combined with the RNA corner motif (RNA+DNA 3,2 ■ and RNA+DNA 3,3 ▼). FRET intensities are plotted as normalized values obtained by subtraction of intensity at $[Mg^{2+}]=0$ (first data point) divided by this same number (fractional difference). Each data point is an average of physical triplicates. Error bars of ±1σ are obscured by the symbols for most data points.

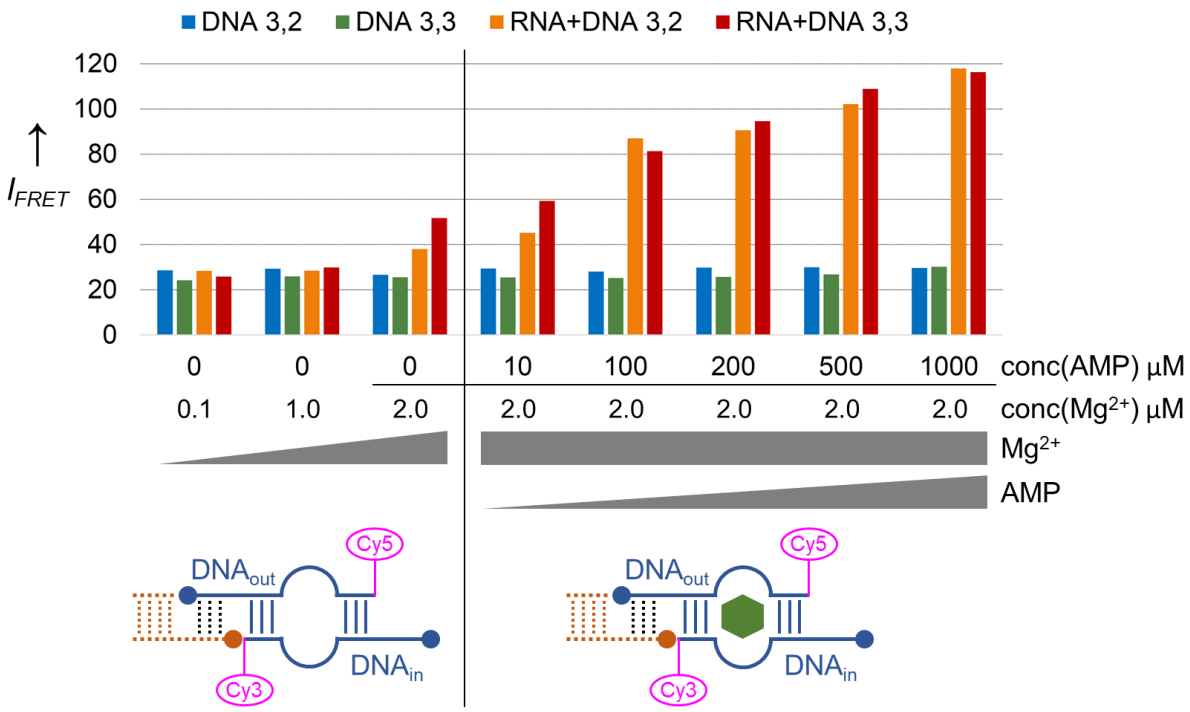

Fig. S9. FRET response in titration of fluorescently labeled nanoshape component mixtures with $MgCl_2$ and AMP ligand. Measurements are shown in groups of four mixtures which contained DNA aptamer variant strands with the FRET dye pair Cy3/Cy5 attached at the 3' terminus of, respectively, DNA_{in} and DNA_{out} (DNA 3,2, blue, and DNA 3,3, green), and the same DNA strands combined with the RNA corner motif (RNA+DNA 3,2, orange and RNA+DNA 3,3, red). FRET intensities are plotted as absolute measured values. The first three groups show FRET response to increased Mg^{2+} concentration up to 2 mM. The following 5 groups show FRET response to increased AMP concentration on a background of 2 mM Mg^{2+}.

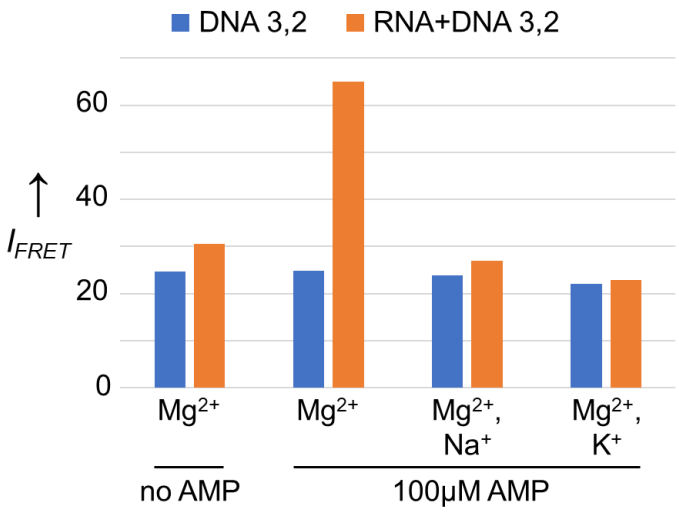

Fig. S10. Impact of monovalent cations on the formation of hybrid nanoshapes containing fluorescently labeled aptamer DNA as monitored by FRET response. Measurements are shown for the DNA 3,2 aptamer variant strands with the FRET dye pair Cy3/Cy5 attached at the 3' terminus of, respectively, DNA_{in} and DNA_{out} (DNA 3,2, blue), and the same DNA strands combined with the RNA corner motif (RNA+DNA 3,2, orange; see also Fig. 5 and ESI Fig. S8). All samples contained 2 mM $MgCl_2$. FRET intensities are plotted as absolute measured values. Samples with monovalent cations contained 100 mM sodium or potassium ions. An increased FRET signal that indicated formation of RNA-DNA aptamer nanostructures was observed only for the combination of all nucleic acid components (RNA corner and DNA aptamer insert) in the presence of both Mg^{2+} and AMP. Consistent with PAGE analysis (ESI Fig. S4), monovalent cations at 100 mM concentration inhibited the formation of the nanostructures as indicated by low FRET signal.

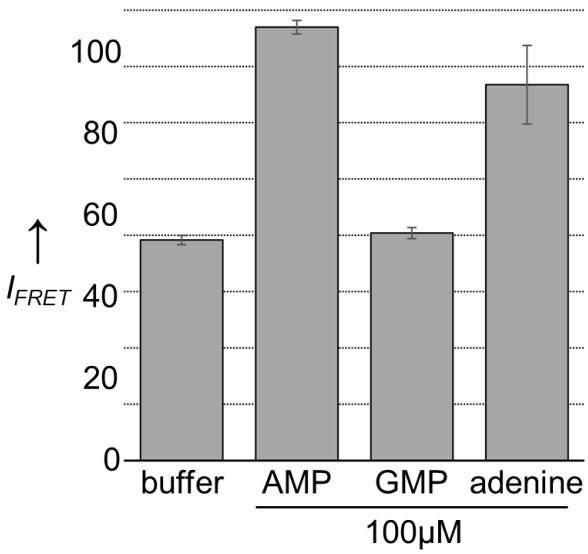

Fig. S11. FRET response of hybrid nanoshapes containing the DNA 3,2 aptamer to different small molecules at 100 μM concentration in the presence of 2 mM magnesium ions. Error bars indicate ±1σ of triplicates tested for each condition.

Table S1. Oligonucleotide sequences

Name	MW g/mole	Sequence
RNA		
RNA_{out}	6107	5’ – rCrGrA rGrArC rCrArG rGrArA rCrUrA rCrUrG rA – 3’
RNA_{in}	4461	5’ – rCrCrG rArGrG rUrCrA rGrCrC rUrG – 3’
DNA		
DNA_{out} Control	5171	5’ – CCT CGG ACG TAC GTA CG – 3’
DNA_{in} Control	5177	5’ – GTC TCG CGT ACG TAC GT – 3’
DNA_{out} 2,2	4954	5’ – CCT CGG CTG GGG GAG T – 3’
DNA_{in} 2,2	4971	5’ – GTC TCG ACG GAG GAA G – 3’
DNA_{out} 2,3	5267	5’ – CCT CGG CTG GGG GAG TA – 3’
DNA_{in} 2,3	5275	5’ – GTC TCG TAC GGA GGA AG – 3’
DNA_{out} 3,2	5258	5’ – CCT CGG TCT GGG GGA GT – 3’
DNA_{in} 3,2	5284	5’ – GTC TCG ACG GAG GAA GA – 3’
DNA_{out} (G_9→T) 3,2	5233	5’ – CCT CGG TCT GGG GTA GT – 3’
DNA_{in} (G_{22}→T) 3,2	5259	5’ – GTC TCG ACG GAG TAA GA – 3’
DNA_{out} 3,3	5572	5’ – CCT CGG TCT GGG GGA GTA – 3’
DNA_{in} 3,3	5589	5’ – GTC TCG TAC GGA GGA AGA – 3’
DNA_{out} (G_9→T) 3,3	5547	5’ – CCT CGG TCT GGG GTA GTA – 3’
DNA_{in} (G_{22}→T) 3,3	5564	5’ – GTC TCG TAC GGA GTA AGA – 3’
DNA_{out} 4,4	6180	5’ – CCT CGG TTC TGG GGG AGT AT – 3’
DNA_{in} 4,4	6215	5’ – GTC TCG ATA CGG AGG AAG AA – 3’
DNA-dye conjugated		
DNA_{out} (Cy5) 3,2		5’ – CCT CGG TCT GGG GGA GT /Cy5/ – 3’
DNA_{in} (Cy3) 3,2		5’ – GTC TCG ACG GAG GAA GA /Cy3/ – 3’
DNA_{out} (Cy5) 3,3		5’ – CCT CGG TCT GGG GGA GTA /Cy5/ – 3’
DNA_{in} (Cy3) 3,3		5’ – GTC TCG TAC GGA GGA AGA /Cy3/ – 3’